Electrostatic Interactions between a Protein and Oppositely Charged Micelles

Patrizia Andreozzi,[†,‡] Adalberto Bonincontro,[‡,§] and Camillo La Mesa*,[†,‡]

Dipartimento di Chimica, SOFT-INFM-CNR Research Center, and CNISM-Dipartimento di Fisica, La Sapienza University, Rome, Italy

Micellar solutions made of a fully fluorinated surfactant, LiPFN, form water-soluble complexes with lysozyme in a wide concentration range. Such complexes are stabilized by electrostatic and, very presumably, double-layer interactions. The mixtures were investigated by combining electrophoretic mobility, DLS, and dielectric relaxation methods. The former gives information on the surface charge density of protein−micelle complexes and indicates that the resulting adducts retain a negative charge (i.e., charge neutralization is incomplete). The double-layer thickness of proteins, micelles, and protein−micelle complexes is also connected to the dielectric relaxation frequency. Changes in particle size (inferred by DLS), charge density, and double-layer thickness are closely interrelated to each other. A model was developed to quantify such properties.

Introduction

The interactions between association colloids and polymers are interesting subjects to the investigator, because of their relevance in many fundamental and applied aspects. Electrostatic interactions between the above objects are ubiquitous and control stabilization, ion binding, charge neutralization, coagulation, flocculation, and phase separation. From a biochemical viewpoint, interest is focused on the stabilization of colloid particles and on their coverage by proteins,[1,2] polysaccharides,[2,3] and polynucleotides.[4] These items are relevant when surface functionalization is required, as in the heparinization of surgical implants.[5]

Proteins are peculiar block polyelectrolytes. Their properties and biochemical activities are sensitive to modifications in charge distribution, subsequent to adsorption onto surfaces. In some cases proteins lose their native conformations and denature.[6,7] Adsorption is concomitant to changes in surface charge density, σ, and in the electrical double layer thickness, $1/\kappa$, of the particles onto which proteins adsorb.[8,9] Thus, the particle physical state, surface functionality, and conformation of an adsorbed biopolymer are strictly interrelated.

From a fundamental viewpoint, micelles and vesicles are much more user-friendly than intrinsic colloids. Studies on such systems offer the opportunity to tune the particle concentration, their size, shape, and charge density. In addition, the soft surfaces peculiar to association colloids are plastic and very similar to biological tissues. That is why micelles and vesicles are used as adsorption sites for biopolymers.[10−16] This possibility opens the way to technological applications, including biomimetic systems used in controlled release and transfection technologies.

The electrochemical behavior of micelles and vesicles is related to the lower or upper limits of the electrical double layer theory, respectively.[17] Micelles and vesicles, in fact, refer to conditions where Hückel (for small) or Smoluchowsky approximations (for large particles) hold. Changes in size, or surface charge density, thus may help in clarifying the double-layer theory in a wide range of colloid particle sizes. In previous work we focused on protein binding onto large synthetic vesicles.[14,16] It is interesting, thus, to investigate the binding of small proteins onto micellar aggregates. In such a case, the protein and micelles are in the size range where Hückel's approximation holds.

In this contribution the interactions between charged micelles and lysozyme are reported and investigation on particle size, electrophoretic mobility, and dielectric relaxation processes are discussed. The ternary system composed of water, lysozyme (LYSO), and lithium perfluorononanoate (LiPFN) is particularly appealing for the above purposes.[18] LiPFN micelles are characterized by small sizes and well-defined surface charge density.[19] The phase diagram of the water−LYSO−LiPFN system has been investigated.[20,21] In such a system molecular solutions, precipitates, protein−surfactant gels, micelle−protein complexes, and micellar solutions are observed, depending on the [protein/surfactant] charge ratio and absolute concentration. Because of their hydrophobic and oleophobic character,[22−25] fluorinated surfactants do not interact with the hydrophobic domains of the protein. Hence electrostatic interactions are dominant in a wide part of the phase diagram. LYSO and oppositely charged micelles exert a mutual electrostatic interaction, which is rationalized here.

Experimental Section

Materials. Chicken egg lysozyme (fraction V, Sigma) was purified as in previous work.[20] Its purity was controlled by the density, ionic conductivity, and viscosity of its aqueous solutions.[26] Lysozyme has eight nominal positive charges in the pH conditions used in this work (≈ 6.5). Unless otherwise indicated, all solutions were prepared in the absence of buffers or without controlling the ionic strength, to avoid drawbacks inherent to modifications in the double-layer thickness of the particles.

Water was doubly distilled in an all-glass apparatus. The ionic conductivity of freshly prepared (carbon dioxide free) water, χ, is $0.7-1.0$ μS cm^{-1} at 25.00 °C.

* Corresponding author. Telephone: +39-06-49913707, +39-06-491694. Fax. +39-06-490631. E-mail: camillo.lamesa@uniroma1.it.
† Dipartimento di Chimica.
‡ SOFT-INFM-CNR Research Center.
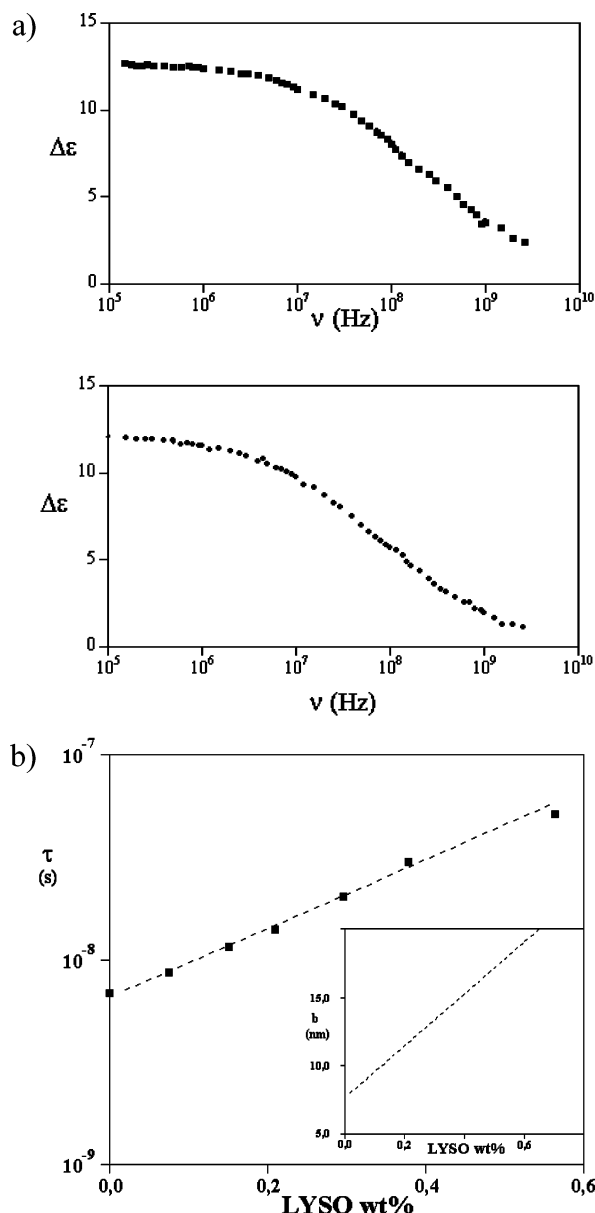§ CNISM-Dipartimento di Fisica.

a)

b)

Figure 1. (A) Dielectric relaxation spectra, relative to a 1.50 wt % surfactant solution at 25.00 °C, up, and to the same mixture with added 0.40 wt % LYSO. (B) Dependence of the relaxation time, τ (s), in semilogarithmic scale, on the amount of added lysozyme to a 1.50 wt % LiPFN micellar solution, at 25.0 °C. The x-axis is proportional to the charge ratio [LYSO/LiPFN]. In the inset is plotted the dielectric radius, b (nm), vs LYSO content, calculated by eq 12.

Lithium perfluorononanoate, LiPFN, was obtained by titration of the corresponding acid (Riedel) with LiOH. The salt was recovered, precipitated in ethanol–acetone mixtures, and vacuum-dried. Conductometric determination of its critical micelle concentration (cmc) in water at 25.00 °C was used as a purity criterion. The ratio of conductivity values above and below the cmc gives estimates of the counterion binding degree[27] and, combined with dynamic light scattering (DLS), of the micelle surface charge density.

Due amounts of the protein were dissolved by weight into 1.50 or 3.00 wt % LiPFN solutions and equilibrated at room temperature for 1 day, in the dark. Samples containing lower, or higher, LiPFN concentrations were used, too. However, they suffered from drawbacks ascribed to the precipitation of complexes, to the width of regions to be investigated, or to the high viscosity, when LiPFN wt % ≥ 3.0. It is worth mentioning that fluorinated surfactants are highly surface active (27–28

TABLE 1: Dielectric Relaxation Time, τ (s), for Different [LYSO/LiPFN] Charge Ratios in a Solution Containing 3.03 wt % LiPFN, at 25.0 °C[a]

[LYSO/LiPFN]	τ (s)
0.00	2.2×10^{-8}
1.51	3.0×10^{-8}
3.02	4.2×10^{-8}
4.19	5.2×10^{-8}
5.93	7.9×10^{-8}
7.90	1.2×10^{-7}
10.0	1.8×10^{-7}

[a] The uncertainty in τ values is ±5%.

mN m^{-1}, or less) and bubbles dispersed therein stand undisturbed for hours, mostly when the mixtures are relatively viscous. This possibility results in disturbing effects on DLS, electrophoretic mobility, and dielectric relaxation.

The samples were stored in a refrigerator. To avoid an undesired precipitation of protein–surfactant complexes, the surfactant was always in excess with respect to the nominal protein charge. The solutions were centrifuged and passed through 0.22 μm filters (Millipore) before being investigated. To avoid the presence of bubbles, they were allowed to stay for some time before measurements were run.

Prolonged electrophoretic mobility experiments modify the appearance of protein-containing mixtures and give colored solutions, or precipitates, depending on protein content, applied voltage, and measuring time. Very presumably, reduction of the S–S bridges onto lysozyme occurs. For the above reasons, mobility measurements were performed for short times, at moderate applied voltages. The final solutions were discarded.

Methods. *Dielectrics.* The dielectric permittivity, ϵ', and loss, ϵ'', were measured at 25.0 °C by HP 4194-A and 4291-A units, working in the range 10^5-10^9 Hz, as indicated elsewhere.[28] Errors on ϵ' values are ±1.0%; those on ϵ'' are ±3.0%. More details on data elaboration and measuring procedures are given elsewhere.[29] The dielectric relaxation frequency, f^*, was obtained by

$$\epsilon^* - \epsilon_\infty = \frac{\Delta\epsilon}{1 + \left(\frac{\mathrm{i}f}{f^*}\right)^{(1-\alpha)}} \qquad (1)$$

where ϵ^* is the complex permittivity, ϵ_∞ is its high-frequency limit, $\mathrm{i} = \sqrt{-1}$, $\Delta\epsilon$ is the dielectric increment, and α is an empirical parameter related to the distribution of relaxation times, usually less than 0.4. Some values are reported in Figure 1A. Selected dielectric relaxation times are reported in Figure 1B and Table 1. Data can be fitted in a single relaxation equation, and the accuracy on the corresponding frequency is always less than 5%. Such errors arise from the fact that micelles and their complexes with proteins or polymers are polydisperse.[30] For more details, see Hasted[31] and references therein.

Electrophoretic Mobility. A laser-velocimetry Doppler utility, Malvern HT-ZS Nano series, determined the electrophoretic mobility, μ (cm^2 V^{-1} s^{-1}), of the protein, of raw micelles, and of protein–micelle complexes. The solutions were located in polystyrene cuvettes equipped with gold electrodes, at 25.0 ± 0.1 °C. The applied voltage was ≤80 V, to avoid the reduction of S–S bridges of LYSO. The apparatus performances were controlled as in previous work.[16] The electrophoretic mobility is transformed into the ζ-potential according to[32]

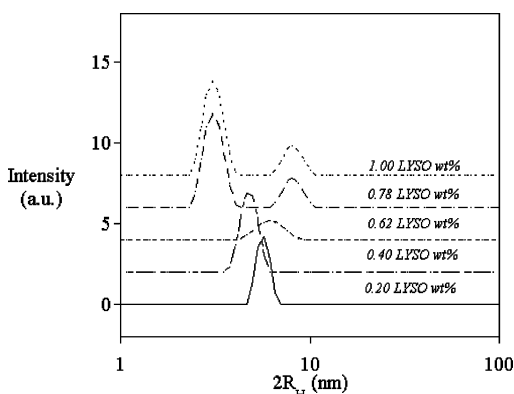$$\zeta = \frac{4\pi\eta\mu}{\epsilon'} \qquad (2)$$

Figure 2. Intensity-based size distribution for concentrations below (solid line) and above the protein−micelle complexation threshold (dotted line) in 1.50 wt % LiPFN, at 25.0 °C. Data are shifted, to avoid overlapping. They are plotted as intensity, I, in a.u., vs particle size, $2r$ (nm), in semilogarithmic scale. The wt % LYSO in the mixtures is indicated in the right-hand side part of each plot.

where ζ is the ζ-potential and η is the solvent viscosity. Nominal errors on ζ values are ± 1.0 mV. The surface charge density, σ, and double-layer thickness, $1/\kappa$, can be interrelated according to

$$\frac{\epsilon' \zeta}{4\pi} = \frac{\sigma}{k} \qquad (3)$$

where the right-hand side term in eq 3 is an electric moment (q/κ) per unit area, A.

DLS. The goniometer was a Brookhaven Model BI-200 SM. An argon ion laser, operating at 514.5 nm and 20 mW, was used. Details on the apparatus, measuring procedures, and data elaboration are given elsewhere.[33−35] The Malvern HT-ZS Nano unit performed DLS measurements in backscattering mode, at 632.8 nm, 173°, and 25.0 ± 0.1 °C. The agreement between particle sizes inferred by the two methods is within a few percent. A CONTIN data analysis facility elaborated the decay-time distribution functions.

Static light scattering (SLS) experiments on pure lysozyme were performed in water−0.10 m NaCl at 25.0 °C. They were elaborated according to

$$\frac{Kc}{R(\theta)} = \frac{P(\theta)}{MW} \sum_{i=2} (1 + A_i c^{(i-1)}) \approx \frac{P(\theta)}{MW} (1 + A_2 c) \qquad (4)$$

where K is a constant, $R(\theta)$ is the ratio between diffuse and incident intensity (depurated by the solvent contribution), $P(\theta)$ is the shape factor, c is its concentration, and MW is its molecular mass.

A_2 in eq 4 was obtained by linearizing the function

$$A_2 = \frac{1}{2\bar{V}_1 (MW)} \int\int \left(\exp\left[-\frac{u(r_1, r_2)}{K_B T}\right] - 1 \right) dr_1\, dr_2 \qquad (5)$$

where $u(r_1, r_2)$ is the interaction potential and $\bar{V}_1$ is the solvent partial molar volume.

No angular resolved SLS experiments could be performed in systems containing free micelles and the protein (i.e., when different scatterers occur). Hence, DLS was used. The field temporal autocorrelation function, $g_1(\tau)$, was derived by

$$g_2(\tau) = \frac{\langle I(t)\, I(t+\tau)\rangle}{\langle I(t)\rangle^2} = 1 + B|g_1(\tau)|^2 \qquad (6)$$

SCHEME 1: Concentric Spheres Model Representing the Dielectric Behavior of Micelles and Their Complexes[a]
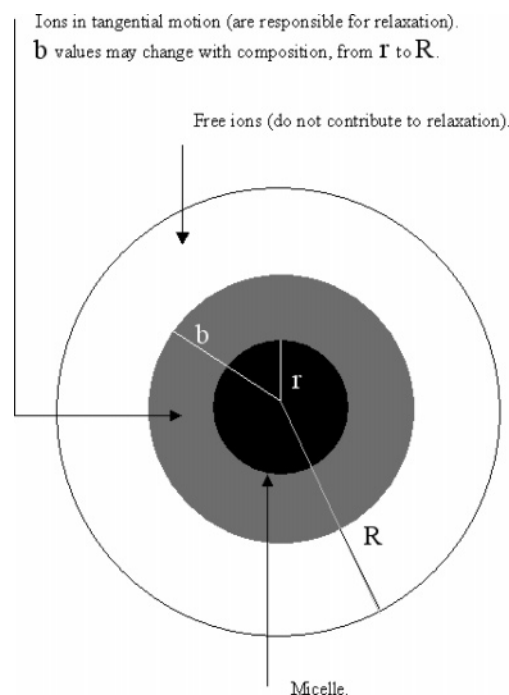
[a] The black inner sphere indicates a micelle, the gray one indicates the region where ions contribute to relaxation, and the empty one refers to the volume where ions are freely moving. Sizes of the different regions are indicated by bars, and b depends on the concentration of added protein.

where $g_2(\tau)$ is the intensity autocorrelation function and B is an instrumental constant.

The following expansion analyzed the $g_1(\tau)$ function:[36]

$$\ln|g_1(\tau)| = -\Gamma_1 \tau + \left(\frac{\Gamma_2}{2}\right)\tau^2 \qquad (7)$$

where Γ_1 and Γ_2 are the first and second cumulants, respectively. Plots of Γ_1 vs the squared scattering vector, q^2, determined the decay of the autocorrelation function. Linear fits in q^2 with an intercept ≈ 0 characterize pure LYSO, pure micelles, and their complexes.

The relaxation processes are due to the particle diffusion, D_{app}, and conform to

$$D_{app} = \frac{\Gamma_1}{q^2} \qquad (8)$$

Finally, D_{app} is related to the particle size by the Stokes−Einstein equation.

Results and Discussion

LiPFN micelles and LYSO are small colloid particles (≈ 5 and 3 nm in diameter, respectively), surrounded by their electrical double layers. As a result of attractive electrostatic interactions between them, an overlapping of the respective double layers occurs, in proper concentration ranges. Accordingly, micelles progressively bind LYSO and their negative surface charge is neutralized, until phase separation, or gelling, occurs.[15,21] Binding depends on the concentration of the two species. In the investigated composition range protein−micelle complexes (about 8 nm in diameter) are formed above a given
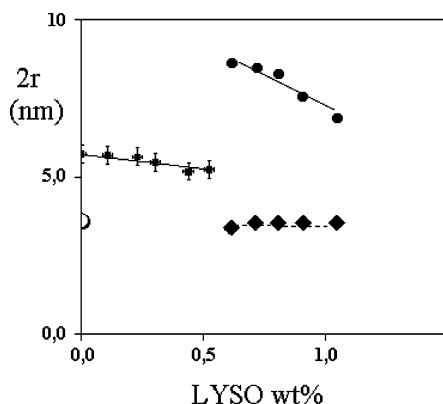
Figure 3. Dependence of $2r$ (nm), inferred by DLS, on amount of protein (in wt %) added to a 1.50 wt % LiPFN solution, at 25.0 °C. The symbol ■ refers to micelles, ● refers to LYSO−micelle complexes, and ◆ refers to free LYSO, respectively. The transition point is the value at which a splitting in two of the scattering populations is observed. The size of bare LYSO is reported as a semicircle in the lower left-hand side of the figure. Data in the region corresponding to the peak broadening are not reported.

Figure 4. Volume fraction (dotted line) and intensity plot (solid line) in arbitrary units, for a selected DLS spectrum, relative to the region where two populations occur. Data refer to a LYSO content of 0.73 wt % in 1.50 wt % LiPFN, at 25.0 °C vs $2r$, in semilogarithmic scale.

[protein/surfactant] charge ratio. No other large scattering entities are observed, as indicated in Figure 2.

In the present experimental conditions, the conformation of bound LYSO is very close to the molten globule state.[37] It is not known whether protein binding and interactions with micelles fulfill the necklace and beads (NB) model, formerly proposed for the water−SDS−LYSO system.[38] In this model the protein adopts a random coil structure and is presumably wrapped around micelles.[39,40] This hypothesis implies the breakup of disulfide bridges and is not consistent with CD data.[37] The interactions between proteins and amphiphilic species rely on the polymer-based or the surfactant-based viewpoint, respectively.[41−43] Each of them suffers from a lack of generality. In the present system the surfactant-based approach is considered, since the protein conformation is not fully clarified.

The income of fluorinated species in the hydrophobic protein tasks is ruled out, since such surfactants are hydrophobic and oleophobic. Simply, they do not like interacting with nonpolar sites of the protein. The interactions are, thus, essentially governed by electrostatics. It is possible that they modify the charge density, size and shape of micelles. To rationalize protein−micelle interactions, the electrostatic attraction between particles, with overlapping of the respective double layers, is considered.

Dielectric Properties. For proteins, the orientational relaxation processes depend on added buffers, or pH.[44] For micellar aggregates, conversely, the interfacial relaxation times are sensitive to surfactant content and added electrolyte. Usually, the relaxation processes of proteins and free micelles occur on very different time scales.[45,46] In the present system, the observed dielectric relaxation, Figure 1A, is due to surfactant aggregates.

An approach to rationalize the dielectric properties of colloid systems, developed by Grosse and Foster,[47,48] was recently modified.[46,49−52] In the theory, large colloid particles are considered as spheres with charges uniformly distributed on their surface. In such a model the charge distribution fulfills Smoluchowsky's approximation and the double-layer thickness is much lower than the particle radius ($\kappa^{-1} \ll r$). The hypothesis that surface conductivity is infinite and relaxation processes are only due to counterion diffusion onto surfaces was modified. Accordingly, the possible relaxation modes are (1) radial,
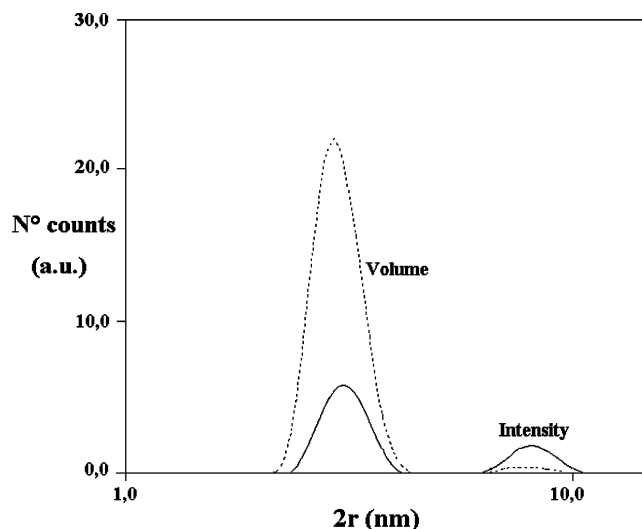
producing polarization effects below the megahertz range, and (2) tangential, concomitant with processes occurring in the 100 MHz range.

The modified Grosse's model was applied to ionic micelles.[46] These are concentric spheres of radius r, surrounded by counterions occupying an electrically neutral volume of radius R. The micelle is surrounded by a layer b ($r < b < R$), containing bound counterions. Ions between b and R do not contribute to relaxation; see Scheme 1. In Hückel's approximation ($\kappa r \approx 1$) the tangential counterion mobility is higher than the radial one and the relaxation time, τ, is

$$\tau = \frac{\tau_b}{3(2 + (2kr/3)^2)} \qquad (9)$$

where $1/k$ is the Debye screening length. τ_b in eq 9 is defined as

$$\tau_b = \frac{b^2}{2D_b} \qquad (10)$$

where D_b is the self-diffusion coefficient of lithium ions.

The dielectric increment is

$$\Delta\epsilon \approx \left(\frac{9 v_b \epsilon_w (2kr/3)^2}{8}\right) \times$$

$$\frac{1 - \frac{2(\sqrt{1 + (2kr/3)^2} - 1)}{3(2kr/3)^2}}{1 + \left(\frac{3}{8}\right)(l - v_b)(2kr/3)^2 + \frac{\sqrt{1 + (2kr/3)^2} - 1}{2}} \qquad (11)$$

where v_b is the ratio $(b/R)^3$.

Estimates of the Debye screening length are inferred by

$$b = r + \kappa^{-1} \qquad (12)$$

where κ^{-1} depends on the micelle charge neutralization due to adsorbed LYSO.[29] Equation 12 applies below the signal splitting observed in Figures 2 and 3.
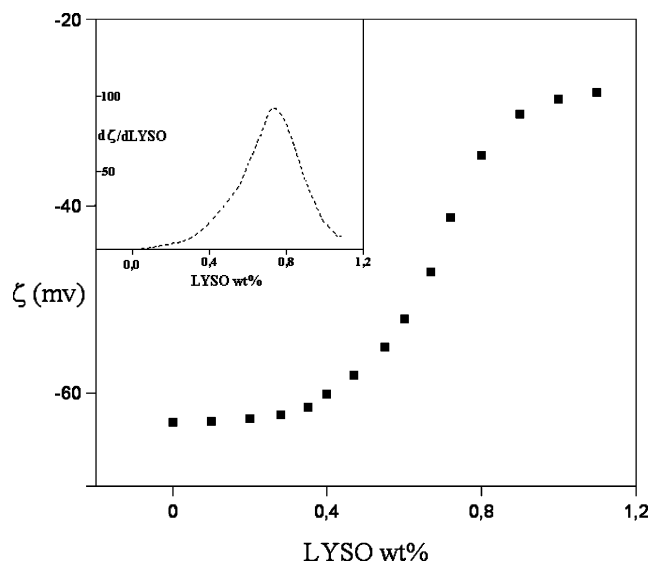
Figure 5. ζ-potential (in mV) vs LYSO wt % of a 1.50 wt % LiPFN micellar solution, at 25.0 °C. In the inset is drawn the derivative of the function. Data below the inflection point were considered in the evaluation of surface charge density.

Figure 6. Surface charge density, σ (q nm^{-2}), vs [LYSO/LiPFN] charge ratio, at 25.0 °C. The LiPFN content is 1.50 wt %. σ values are reported in modulus, to draw an exponential decay fit.

The relaxation processes in Figure 1A (and in Table 1, as well) refer to the real permittivity, due to the tangential motion of counterions. Assuming D_b to be 1.33 10^{-9} m^2 s^{-1} for Li$^+$,[53] the dielectric radius of micelles can be evaluated by combining eqs 9 and 10. The relaxation amplitude inferred by eq 11 is consistent with the experimentally observed one. Accordingly, the approach indicates that the relaxation time and amplitude of micellar solutions are sensitive to the micelle charge density, i.e., to the addition of LYSO.

The diameter of bare LiPFN micelles by DLS, r, ranges between 4.7 and 5.3 nm. Conversely, b values refer to charged spheres surrounded by ion clouds partly neutralized from the protein (Figure 1B). They contain information on the Debye screening length of micelles or micelle−protein complexes and are obtained by assuming micelles as globular polyelectrolytes coexisting with free LYSO, lithium ions, and molecular surfactant.[29] Micelle diameters by DLS, conversely (Figure 3), are always lower than b ones. Comparison of r values with b ones, thus, allows estimation of the double-layer thickness. The values of b increase on increasing LYSO content, in proportion to the charge neutralization by the protein. This is a consequence of the reduced charge density of micelles interacting with LYSO.

Light Scattering. The size of the raw protein in water−0.1 m NaCl (about 3.3 nm) is very close to that formerly reported by SAXS and DLS[54] and does not need to be discussed here. As to bare LiPFN micelles, no comparison can be made with literature data, although SANS and NMR self-diffusion experiments have been reported on systems containing similar species.[55,56] The size of bare LiPFN micelles is consistent with studies mentioned above. (N.B.: The hydrodynamic radii from NMR are consistent with DLS ones only when comparison between z-average and number-average statistics is possible.[35]) It is assumed, accordingly, that LiPFN micelles are about 5 nm in diameter.

As to the mixed protein−surfactant systems, two different regimes are observed in Figure 2. At low [protein/surfactant] charge ratios, micelles adsorb tiny amounts of LYSO. For such ratios, only one population of scattering entities is observed. The peak centered around 5 nm in Figure 2 is ascribed to free micelles. Its average size does not depend on LYSO concentration. However, when the protein content in the medium exceeds
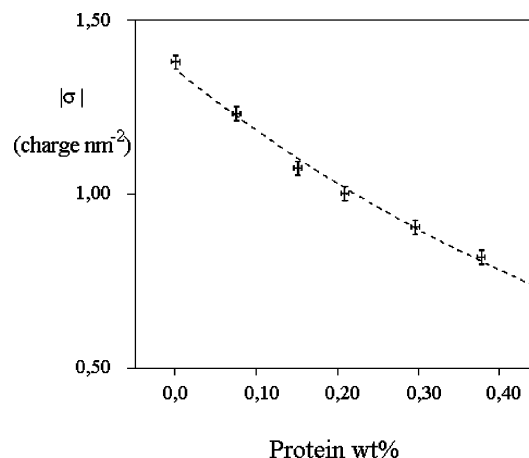
0.65 wt %, two scattering populations are observed, with the occurrence of small and large particles (Figure 3). Larger particles are presumably protein−micelle complexes. The small particles observed above the transition point are, very presumably, surfactant-depleted lysozyme molecules. Accordingly, protein−micelle complexes are the result of a chemical equilibrium between free and bound states and the stoichiometry of the complex depends on [LYSO/micelle] charge ratio. When the protein concentration increases, a splitting of the original peak in two is observed. Support for these findings comes from studies on the water−lysozyme−SDS system.[57] Almgren et al. showed that lysozyme−SDS complexes are formed when the protein content increases. They also observed a splitting of the DLS time correlation function in two. The similarity with our results is, thus, remarkable.

The relative amount of LYSO−LiPFN complexes in the medium can be evaluated by analyzing DLS data in terms of volume fraction statistics (Figure 4). The fit indicates the ceexistence of free LYSO with large scatterers (the complexes). At the onset of such a composition range the system contains about 80 LiPFN molecules per protein. Presumably, protein−micelle complexes are anisometric in shape. Unexpectedly, the complexes reduce in size upon addition of further amounts of LYSO, since the formation of complexes is counteracted by the hindrance between different protein molecules bound onto micelles and by electrostatic interactions as well. It is worth noticing that SANS data relative to micelles in gels made of LYSO and SDS indicate the occurrence of a complicated growth mechanism.[58]

ζ-**Potential.** Electrophoretic mobility plots, reported in Figure 5, show a pronounced change in slope at LYSO content close to that observed in DLS experiments. This behavior is concomitant to a partial charge neutralization. Above the inflection point changes in ζ-potential are less significant, as shown by the inset of Figure 5. Anyhow, the surface charge density of the complexes is far from full neutralization.

In the following efforts are made to relate dielectric and DLS experiments to ζ-potential ones at concentrations below the inflection threshold. We evaluate protein binding in the linear regime (for low [LYSO/micelle] charge ratios) and compare it with the corresponding dielectric data. In the linear regime of Figure 5, the ζ-potential decreases in proportion to the surface charge density. In the same time, the double-layer thickness increases and mobile charges are depleted from the micelle surface. When σ/κ approaches zero, the ζ-potential is null,[14]

the net charge on the particle surface goes to zero, and the double-layer thickness diverges. Charge neutralization implies phase separation and no correlation between particles and their counterions. This is the physical meaning of eq 3. It is possible to evaluate σ and k^{-1} values, by combining eqs 3 and 12. As mentioned above, this approximation holds only for one scattering population. The results indicate that σ regularly decreases with LYSO content (Figure 6) and the nominal charge per unit area significantly decreases, as expected.

Some more aspects must be considered. First, the charge per unit area onto micelles is ≈ 1.4 q nm^{-2}. Such a value is close to that of fluorinated micelles, whose area per molecule is about 0.7 nm^2.[59] Moreover, the significant reduction of surface charge density is reasonable, given the possibility for LYSO to neutralize different binding sites. The size of protein−micelle complexes depends on the concentration of the two species and slightly decreases with LYSO content. It is not easy, in fact, to arrange many protein molecules onto micelles without having significant electrostatic repulsions between them.

Conclusions

Electrostatic interactions between oppositely charged proteins and micelles were considered. LYSO was mixed with aggregates made of a fully fluorinated surfactant, and the resulting interactions were evaluated by DLS, dielectric relaxation, and ζ-potential. As a result of such interactions, the formation of protein−micelle complexes occurs. The process is governed by the relative amounts of the components, and complex formation occurs above a certain threshold.

The interactions are concomitant to a reduction in the surface charge density of micelles up to formation of complexes. Given the difficulty of dealing with systems containing different particles (micelles, protein, and their complexes), the analysis refers to the linear perturbation regime, when LYSO content is low. In this region the surface charge density of the aggregates regularly decreases with protein content, because of a partial charge neutralization.

In the Hückel regime the screening length is comparable in size to that of the interacting colloids. The agreement between dielectric relaxation and ζ-potential findings is significant. This is documented by changes in the surface charge density of micelles before the formation of protein−micelle complexes. Compared to other systems made of large vesicles and globular proteins,[13] there are both differences and similarities. Micelles are smaller in size and have higher charge densities than vesicles. The adsorption of proteins therein is governed by excluded-volume and electrostatic effects.

In dielectric relaxation processes Cole−Cole plots allow dealing with polydisperse systems, whose width is modulated by the α parameter. The latter quantity is related to a distribution of dynamic events in a relatively narrow window. It is worth noticing, finally, the excellent convergence of DLS, electrophoretic mobility, and dielectric relaxation experiments. They give an exhaustive description of processes occurring at interfaces and reasonable estimates of the Debye screening length, which is subsequent to modifications in surface charge density. The present approach arises from the combination of different methods and can be used as a standard protocol in the evaluation of charge modifications of small colloids.

References and Notes

(1) Li, D.; Teoh, W. Y.; Selomulya, C.; Woodward, R. C.; Amal, R.; Rosche, B. *Chem. Mater.* **2006**, *18*, 6403.
(2) Duchesne, L.; Fernig, D. G. *Anal. Biochem.* **2007**, *362*, 287.
(3) Gu, M.-Q.; Yuan, X.-B.; Kang, C.-S.; Zhao, Y.-H.; Tian, N.-J.; Pu, P.-Y.; Sheng, J. *Carbohyd. Polym.* **2007**, *67*, 417.
(4) Rittich, B.; Spanova, A.; Horak, D.; Benes, M. J.; Klesnilova, L.; Petrova, K.; Rybnikar, A. *Colloids Surf., B: Biointerfaces* **2006**, *52*, 143.
(5) Guo, J.; Amemiya, S. *Anal. Chem.* **2006**, *78*, 6893.
(6) Li, D.; Teoh, W. Y.; Selomulya, C.; Woodward, R. C.; Amal, R.; Rosche, B. *Chem. Mater.* **2006**, *18*, 6403.
(7) Lundqvist, M.; Sethson, I.; Jonsson, B.-H. *Langmuir* **2005**, *21*, 5974.
(8) Maheshwari, R.; Dhathathreyan, A. *J. Colloid Interface Sci.* **2006**, *293*, 263.
(9) Shamin, N.; Hong, L.; Hidajat, K.; Uddin, M. S. *J. Colloid Interface Sci.* **2006**, *304*, 1.
(10) Mel'nikov, S. M.; Dias, R.; Mel'nikova, Y. S.; Marques, E. F.; Miguel, M. G.; Lindman, B. *FEBS Lett.* **1999**, *453*, 113.
(11) Marques, E. F. *Langmuir* **2000**, *16*, 4798.
(12) Jung, H. T.; Coldren, B.; Zasadzinski, J. A.; Iampietro, D. J.; Kaler, E. W. *Proc. Natl. Acad. Sci. U.S.A.* **2001**, *98*, 1353.
(13) Marques, E. F.; Regev, O.; Khan, A.; Miguel, M. G.; Lindman, B. *J. Phys. Chem. B* **1998**, *102*, 6746.
(14) Letizia, C.; Andreozzi, P.; Scipioni, A.; La Mesa, C.; Bonincontro, A.; Spigone, E. *J. Phys. Chem. B* **2007**, *111*, 898.
(15) Ciurleo, A.; Cinelli, S.; Guidi, M.; Bonincontro, A.; Onori, G.; La Mesa, C. *Biomacromolecules* **2007**, *8*, 399.
(16) Bonincontro, A.; Spigone, E.; Ruiz-Pena, M.; La Mesa, C. *J. Colloid Interface Sci.* **2006**, *304*, 342.
(17) Hiemenz, P. C. *Principles of Colloid and Surface Chemistry*, 2nd ed.; Marcel Dekker: New York, 1986; Chapter XII, p 677.
(18) Muzzalupo, R.; Ranieri, G. A.; La Mesa, C. *Colloids Surf., A: Physicochem. Eng. Aspects* **1995**, *104*, 327.
(19) La Mesa, C.; Sesta, B. *J. Phys. Chem.* **1987**, *91*, 1450.
(20) Palacios, A. C.; Sarnthein-Graf, C.; La Mesa, C. *Colloids Surf., A: Physicochem. Eng. Aspects* **2003**, *228*, 25.
(21) Sesta, B.; Gente, G.; Iovino, A.; Laureti, F.; Michiotti, P.; Paiusco, O.; Palacios, A. C.; Persi, L.; Princi, A.; Sallustio, S.; Sarnthein-Graf, C.; Capalbi, A.; La Mesa, C. *J. Phys. Chem. B* **2004**, *108*, 3036.
(22) Gente, G.; La Mesa, C.; Muzzalupo, R.; Ranieri, G. A. *Langmuir* **2000**, *16*, 7914.
(23) Kunieda, H.; Shinoda, K. *J. Phys. Chem.* **1976**, *80*, 2468.
(24) Hoffmann, H.; Schorr, W. *J. Phys. Chem.* **1981**, *85*, 3160.
(25) Mukerjee, P.; Korematsu, K.; Okawauki, M.; Sugihara, G. *J. Phys. Chem.* **1985**, *89*, 5308.
(26) Monkos, K. *Biochim. Biophys. Acta: Protein Struct. Mol. Enzymol.* **1997**, *1339*, 304.
(27) Muzzalupo, R.; Ranieri, G. A.; La Mesa, C. *Colloids Surf., A: Physicochem. Eng. Aspects* **1995**, *104*, 327.
(28) Bonincontro, A.; Briganti, G.; Giansanti, A.; Pedone, F.; Risuleo, G. *Colloids Surf., B: Biointerfaces* **1996**, *6*, 219.
(29) Bonincontro, A.; Michiotti, P.; La Mesa, C. *J. Phys. Chem. B* **2003**, *107*, 14164.
(30) D'Aprano, A.; La Mesa, C.; Persi, L. *Langmuir* **1997**, *13*, 5876.
(31) Hasted, J. B. *Aqueous Dielectrics*; Chapman & Hall: London, U.K., 1973; Chapter I, p 25.
(32) Adamson, A. W. *Physical Chemistry of Surfaces*, 5th ed.; Wiley: New York, 1990; Chapter V, p 218.
(33) Pede, S.; Galantini, L.; La Mesa, C.; Capitani, D.; Segre, A. L. *Colloid Polym. Sci.* **2007**, *285*, 1067.
(34) Sallustio, S.; Galantini, L.; Gente, G.; Masci, G.; La Mesa, C. *J. Phys. Chem. B* **2004**, *108*, 18876.
(35) D'Archivio, A. A.; Galantini, L.; Tettamanti, E. *J. Phys. Chem. B* **2000**, *104*, 9255.
(36) Koppel, D. E. *J. Chem. Phys.* **1972**, *57*, 4814.
(37) Turro, N. J.; Lei, X.-G.; Ananthapadmanabhan, K. P.; Aronson, M. *Langmuir* **1995**, *11*, 2525.
(38) Sogami, M.; Era, S.; Koseki, T.; Nagai, N. *J. Peptide Res.* **1997**, *50*, 465.
(39) Shirahama, K.; Tsuji, K.; Tagali, T. *J. Biochem.* **1974**, *75*, 309.
(40) Chen, S. H. *Phys. Rev. Lett.* **1986**, *57*, 2583.
(41) *Interactions of Surfactants with Polymers and Proteins*; Goddard, E. D., Ananthapadmanabhan, P., Eds.; CRC Press: Boca Raton, FL, 1992.
(42) *Polymer Surfactant Systems*; Kwak, J. C. T., Ed.; Surfactant Science Series; Marcel Dekker: New York, 1998.

(43) Holmberg, K.; Jonsson, B.; Kronberg, B.; Lindman, B. *Surfactants and Polymers in Aqueous Solutions*, 2nd ed.; Wiley: New York, 2002.

(44) Bonincontro, A.; De Francesco, A.; Onori, G. *Colloids Surf., B: Biointerfaces* **1998**, *12*, 1.

(45) Bonincontro, A.; De Francesco, A.; Onori, G. *Chem. Phys. Lett.* **1999**, *301*, 189.

(46) Barchini, R.; Pottel, R. *J. Phys. Chem.* **1994**, *98*, 7899.

(47) Grosse, C.; Foster, K. R. *J. Phys. Chem.* **1987**, *91*, 6415.

(48) Grosse, C. *J. Phys. Chem.* **1988**, *92*, 3905.

(49) Shikata, T.; Imai, S. I. *Langmuir* **1998**, *14*, 6804.

(50) Imai, S. I.; Shikata, T. *Langmuir* **1999**, *15*, 8388.

(51) Baar, C.; Buchner, R.; Kunz, W. *J. Phys. Chem. B* **2001**, *105*, 2906.

(52) Imai, S. I.; Shiokawa, M.; Shikata, T. *J. Phys. Chem. B* **2001**, *105*, 4495.

(53) Egorov, A. V.; Kornolkin, A. V.; Chizhic, V. I.; Yushmanov, P. V.; Lyubartsev, A. P.; Laaksonen, A. *J. Phys. Chem. B* **2003**, *107*, 3234. (N.B.: Data reported therein refer to a temperature of 33.0 °C.)

(54) Leggio, C.; Galantini, L.; Zaccarelli, E.; Pavel, N. V. *J. Phys. Chem. B* **2005**, *109*, 23857.

(55) Pedone, L.; Chillura Martino, D.; Caponetti, E.; Floriano, M. A.; Triolo, R. *J. Phys. Chem. B* **1997**, *101*, 9525.

(56) Petrov Bossen, D.; Matsumoto, M.; Nakamura, M. *J. Phys. Chem. B* **1999**, *103*, 8251.

(57) Valstar, A.; Brown, W.; Almgren, M. *Langmuir* **1999**, *15*, 2366.

(58) Stenstam, A.; Montalvo, G.; Grillo, I.; Gradzielski, M. *J. Phys. Chem. B* **2003**, *107*, 12331.

(59) Sesta, B.; Segre, A. L.; D'Aprano, A.; Proietti, N. *J. Phys. Chem. B* **1997**, *101*, 198.